DNA Nanotechnology | Very Important Paper

How to cite: *Angew. Chem. Int. Ed.* **2020**, *59*, 20577–20581
International Edition: doi.org/10.1002/anie.202008553
German Edition: doi.org/10.1002/ange.202008553

Protein-Controlled Actuation of Dynamic Nucleic Acid Networks by Using Synthetic DNA Translators**

Alessandro Bertucci, Alessandro Porchetta, Erica Del Grosso, Tania Patiño, Andrea Idili, and Francesco Ricci**

Abstract: *Integrating dynamic DNA nanotechnology with protein-controlled actuation will expand our ability to process molecular information. We have developed a strategy to actuate strand displacement reactions using DNA-binding proteins by engineering synthetic DNA translators that convert specific protein-binding events into trigger inputs through a programmed conformational change. We have constructed synthetic DNA networks responsive to two different DNA-binding proteins, TATA-binding protein and Myc-Max, and demonstrated multi-input activation of strand displacement reactions. We achieved protein-controlled regulation of a synthetic RNA and of an enzyme through artificial DNA-based communication, showing the potential of our molecular system in performing further programmable tasks.*

Introduction

Information processing in living systems relies on the communication between different biomolecules. The whole genetic machinery, for example, is based on the dynamic interplay between proteins, DNA and RNA: direct protein-DNA communication is achieved by DNA-binding proteins such as transcription factors that recognize specific DNA domains called consensus sequences and regulate the rate of transcription of genes into messenger RNA.[1] In an effort to artificially recreate Nature's language, DNA nanotechnology has translated the governing principles of nucleic acid hybridization into programmable bioinspired systems that can be tuned in space and time.[2–4] Toehold-mediated strand displacement is arguably the most simple, robust and versatile tool available to generate dynamic, responsive and transformative higher-order networks in which synthetic DNA oligonucleotides perform programmable tasks with possible applications in synthetic biology, sensing and information processing.[5–10] However, nucleic acid trigger inputs are generally required for upstream activation: this ultimately limits the extent to which DNA-based computation can mediate artificial communication between different species.

Strand displacement reactions actuated by proteins are challenging because they require the implementation of non-trivial binding-induced mechanisms. One clever strategy makes use of proteins as substrates that promote molecular interactions in a confined volume and induce the hybridization between complementary DNA strands through the increase of their local concentration.[11–16] This strategy is however limited by the availability of specific affinity ligands that must be conjugated to the interacting DNA strands and by the need of multiple binding sites on the target protein. Alternatively, protein-responsive sensing technologies and DNA-based architectures have been engineered capitalizing on the natural DNA binding activity of transcription factors.[17–21] This approach is particularly appealing as it allows direct protein-DNA communication bypassing the use of affinity ligands; nevertheless, to date, it has never been interfaced with dynamic synthetic DNA systems and harnessed to control DNA-based computation.

Motivated by the above considerations, we report here the rational design of synthetic DNA translators that convert an input protein-binding event into the output activation of an arbitrary biomolecular system (Figure 1). We demonstrate that it is possible to tune the output of dynamic DNA networks and to perform multi-input operations using proteins as biochemical inputs and we show that DNA-mediated, artificial communication pathways can be established to allow non-natural regulation of RNA and protein functionality.

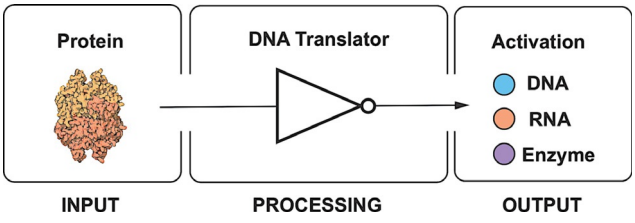

Figure 1. Schematic overview of the artificial communication pathway mediated by a DNA translator that converts a specific protein binding event into the downstream activation of different biomolecular systems.

[*] Dr. A. Bertucci, Dr. A. Porchetta, Dr. E. Del Grosso, Dr. T. Patiño, Prof. F. Ricci
Department of Chemistry, University of Rome Tor Vergata
Via della Ricerca Scientifica, 00133 Rome (Italy)
E-mail: alessandro.bertucci@uniroma2.it
francesco.ricci@uniroma2.it

Dr. A. Idili
Catalan Institute of Nanoscience and Nanotechnology (ICN2)
Campus UAB, Bellaterra, 08193 Barcelona (Spain)

[**] A previous version of this manuscript has been deposited on a preprint server (https://doi.org/10.26434/chemrxiv.12424658.v1).

Supporting information and the ORCID identification number(s) for the author(s) of this article can be found under: https://doi.org/10.1002/anie.202008553.

Results and Discussion

Our protein responsive DNA translator is a synthetic DNA sequence encoding the double stranded consensus sequence specifically recognized by a DNA-binding protein and a single stranded input sequence able to initiate a toehold strand displacement reaction. We have rationally designed such DNA translator to be in a thermodynamic equilibrium between two mutually exclusive conformations. The first structure, more stable, is a double-hairpin structure in which the two portions encoding the double stranded consensus sequence are physically separated and form two loop regions (red domains, Figure 2a). In this conformation the toehold-binding region of the input strand sequence (orange domain, Figure 2a) is incorporated into one of the two duplex portions so that it is unable to initiate the strand displacement reaction. The second, less favorable, structure is a hairpin conformation in which the double stranded consensus sequence is fully formed and the input strand is free to initiate a strand displacement reaction. The presence of a specific DNA-binding protein recognizing its cognate consensus sequence in the DNA translator is then expected to shift such thermodynamic equilibrium towards the second "active" conformation through a population-shift mechanism.[18,22] We initially designed a DNA translator responsive to TATA binding protein (TBP), a transcription factor ubiquitously present in eukaryotic cells.[23] The thermodynamic switching equilibrium constant (K_S) of the DNA translator determines the TBP-induced conformational transition and therefore will affect the efficiency of the strand displacement reaction. In order to optimize the input-output behavior, we have then engineered a set of five TBP-responsive translators (TBP-Translators)

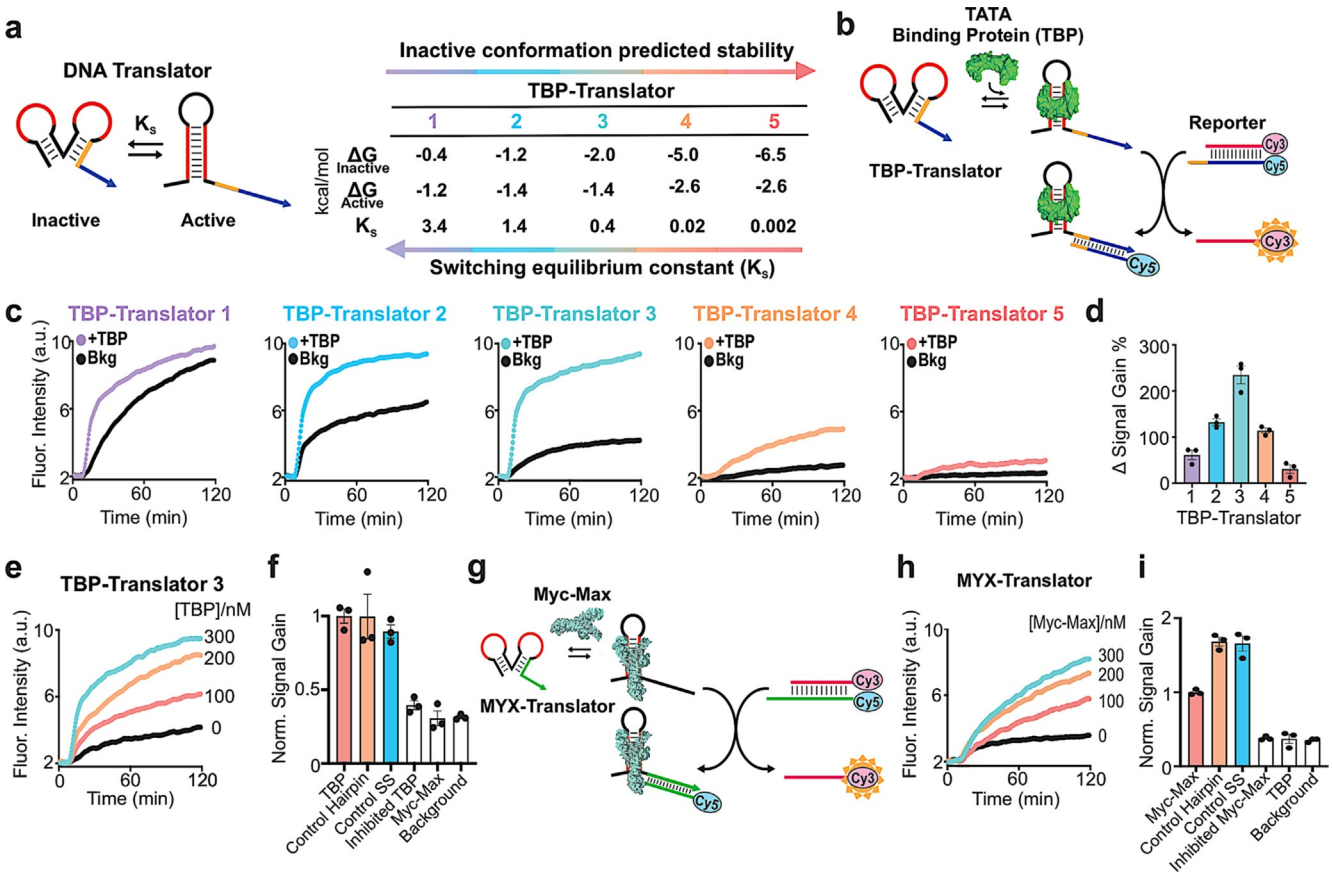

Figure 2. a) A TBP-controlled DNA translator (TBP-Translator) is in thermodynamic equilibrium between two mutually exclusive conformations (active and inactive). The table reports the predicted thermodynamic stability and switching equilibrium constant (K_S) of the two conformations for a set of different TBP-Translators. b) TBP-actuated strand displacement using the TBP-Translator. c) Kinetic profiles of strand displacement reactions in the presence (+TBP) or absence (Bkg) of TBP (300 nM) obtained in an equimolar solution of TBP-Translator and reporter duplex (30 nM). d) ΔSignal Gain % obtained for each TBP-Translator, calculated as the difference between the signal gain % of the TBP-controlled reaction and the one relative to the background ($n=3$, mean + standard error of the mean, SEM). e) Modulation of the strand displacement output signal using TBP-Translator 3 in presence of different concentrations of TBP. f) Normalized signal gains obtained with TBP (300 nM), a control hairpin invader (Control hairpin, 30 nM) and a single-stranded invader (Control SS, 30 nM). Signal gains observed with TBP in the presence of saturating concentrations of the consensus sequence (Inhibited TBP) and with a non-specific protein (i.e. Myc-Max, 300 nM) are also shown together with the background signal ($n=3$, mean + SEM). g) Myc-Max-actuated strand displacement using a Myc-Max-responsive DNA translator (MYX-Translator). h) Modulation of the strand displacement output signal using MYX-Translator in the presence of different concentrations of Myc-Max. i) Normalized signal gains obtained with Myc-Max (300 nM), a control hairpin invader (30 nM) and a single-stranded invader (30 nM). Signal gains observed with Myc-Max in the presence of saturating concentrations of the consensus sequence (Inhibited Myc-Max) and with a nonspecific protein (i.e. TBP, 100 nM) are also shown together with the background signal ($n=3$, mean + SEM).

with different predicted switching equilibrium constants K_S (Figure 2a, full sequences reported in the SI). More specifically, we rationally varied the GC/AT content of the translator portions not involved in the protein recognition event to finely tune the predicted standard free energies of the two switching conformations (Figure SI1). As a reporter system of the strand displacement reaction, we used a DNA duplex (30 nM) equipped with an optical pair (Cy3-Cy5) and monitored the progression of the strand displacement reaction over time by following the increase in Cy3 fluorescence intensity (Figure 2b). Each of the five TBP-Translators was tested in the absence and presence of input TBP. The translators showed different degrees of background signal, caused by the uncontrolled initiation of the strand displacement reaction, as a result of their varying thermodynamic stabilities (Figure 2c). The best trade-off between TBP-induced strand displacement and non-specific background (Δ*S*ignal Gain % $= 235 \pm 19$) was achieved using the TBP-Translator 3 ($K_S = 0.4$) (Figure 2d and SI2). We note that, on the basis of the current molecular design and the intrinsic switching equilibrium of the translator, a background strand displacement reaction is thermodynamically inevitable. A reduction of the background may be obtained by designing more advanced leakless DNA circuits, by engineering dynamic networks supplemented with transient chemical fuels, or by creating sophisticated communication systems enabled by spatial compartmentalization of the reactive species in which threshold signals can be finely controlled.[24] We thus focused on the TBP-Translator 3 for a further characterization of the system. By using different concentrations of TBP in the 100–300 nM range, it was possible to finely modulate the extent of the strand displacement reaction (Figure 2e). The efficiency of the TBP-responsive strand displacement reaction was evaluated by benchmarking against the fluorescence outputs obtained using equivalent concentrations of either a single stranded input sequence (Control SS, Figure 2f) or a hairpin structure mimicking the TBP-Translator active conformation when bound to TBP (Control hairpin, Figure 2f), and no significant differences were found. Additionally, the great similarity observed between the kinetic profiles of the strand displacement reactions obtained using either the TBP-Translator 3 in the presence of TBP or the above control hairpin sequence, respectively, suggests that the downstream strand displacement process can be assumed as the rate-determining step of the kinetics of the whole system (Figure SI3). To have further validation of the binding-induced mechanism underlying the strand displacement reaction, we ran a competitive assay in which we pre-incubated TBP with an excess of a DNA hairpin bearing the complete TBP-binding domain. In this case, TBP-mediated strand displacement reaction did not occur, and we only registered a signal indistinguishable from the background signal (Figure 2f and SI4). This also seems to suggest that competitive binding strategies might be devised to enable recycling of a bound DNA translator so that the system could be operated in a reversible manner. Additional proof of the interaction between TBP and TBP-Translator 3 was achieved by conducting a gel electrophoresis analysis of the mono- and multi-molecular species involved in the strand displacement reaction (Figure SI5). The TBP-Translator is also specific: no signal was observed with an unrelated DNA-binding protein recognizing a different consensus sequence (Myc-Max, Figure 2f and SI6).

In order to demonstrate the generality of our approach, we rationally designed a DNA translator responsive to Myc-Max complex, another transcription factor that is clinically relevant in oncology.[25] We have engineered this Myc-Max-responsive DNA translator, hereafter referred to as MYX-Translator, following the design rules conducted with the previously described TBP-controlled system (Figure 2g, SI7). More specifically, we have rationally designed a translator that interconverts between two mutually exclusive active and inactive conformations, respectively, with a predicted K_S of 0.4. The Myc-Max-controlled strand displacement reaction observed with this translator in presence of a saturating concentration of the target protein provided a Δ*S*ignal Gain % of 169 ± 39, with a signal-to-noise ratio of 2.0 ± 0.4 (Figure SI6). Varying the concentration of Myc-Max allowed for modulating the strand displacement output, similarly to what observed with the TBP-controlled system (Figure 2h). The Myc-Max-actuated process yielded around 75% of the signal obtained using comparable concentrations (30 nM) of either a control single-stranded input sequence or a hairpin structure mimicking the active MYX-Translator conformer (Figure 2i). This lower relative efficiency may be ascribed to a less effective binding of Myc-Max to the MYX-Translator compared to that of TBP to its cognate translator (Figure 2f), or a less efficient strand invasion process possibly caused by steric hindrance effects.[26] Pre-incubation of Myc-Max with an excess of a DNA hairpin displaying the double stranded Myc-Max consensus sequence resulted in the inhibition of the Myc-Max-induced strand displacement reaction (Figure 2i and SI8). To investigate cross-reactivity, we exposed the Myc-Max-controlled network to TBP. We found that exposure to TBP 100 nM generated signals not significantly different from the background (Figure 2i and SI9). Our protein-controlled DNA translators specifically respond to their cognate input proteins and allow the orthogonal activation of strand displacement reactions in a multi-strand DNA system. To demonstrate this, we designed a multi-input network presenting simple binary logic composed of two reporter DNA duplexes (30 nM) with distinct fluorescence emission windows and responsive to two different protein-actuated DNA translators, that is, TBP and Myc-Max (Figure 3 and Figure SI10). Our molecular network can be orthogonally controlled in the same solution by TBP and Myc-Max in a programmable, multi-input manner (Figure 3).

To further investigate the capability of our platform to support advanced DNA-based computation and to enable artificial communication between non-naturally related biomolecules, we set out to perform protein-induced activation of a functional RNA structure. To do this, we focused on a synthetic fluorogenic RNA aptamer (Mango III) that yields a bright fluorescence signal upon binding to a thiazole orange (TO-1) dye.[27,28] We prevented folding of such RNA aptamer into its optically active conformation by using a blocking RNA strand that hybridizes to a critical region of the aptamer. Displacement of the blocking strand operated by an ad hoc

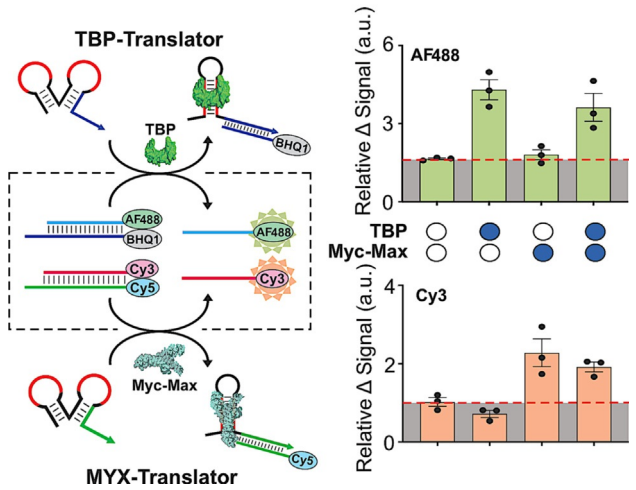

Figure 3. A TBP-responsive strand displacement reaction produces a fluorescence maximum at $\lambda = 516$ nm (AF488) while a Myc-Max-responsive system peaks at $\lambda = 565$ nm (Cy3). The two networks are orthogonally controlled in the same solution using the relevant protein inputs (TBP 100 nM, Myc-Max 300 nM). The relative ΔSignal is the difference between the fluorescence intensity at $t = 60$ min and the initial fluorescence signal of each reporter duplex ($n = 3$, mean + SEM).

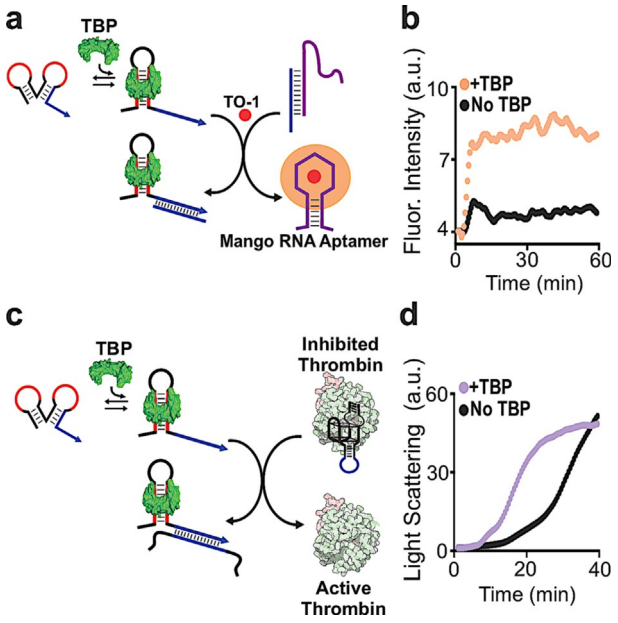

Figure 4. a) Schematic representation of TBP-controlled activation of a fluorogenic RNA Mango aptamer. b) Mango-based fluorescence signal with (+TBP) or without (No TBP) the addition of TBP (1 μM) to a solution containing 100 nM of TBP-Mango-Translator and 30 nM of blocking RNA/Mango aptamer complex. c) Schematic representation of TBP-controlled regulation of the proteolytic activity of thrombin. d) Intensity of light scattering due to thrombin-generated fibrin aggregates in the presence (+TBP) or absence (No TBP) of TBP (300 nM) in a solution containing equimolar concentration of TBP-Thrombin-Translator and thrombin aptamer (50 nM) and thrombin (1 nM).

designed TBP-activated DNA translator (TBP-Mango-translator) allows the correct folding of the active RNA aptamer structure, which generates a fluorescence signal (Figure 4a).[29]

Using 100 nM of TBP-Mango-translator in the presence of TBP (600 nM), we successfully achieved TBP-controlled folding and activation of the Mango aptamer (Figure 4b). Of note, the TBP-induced Mango activation process was as efficient as when using a stable DNA hairpin structure mimicking the active conformation of the TBP-Mango-translator (Figure SI11).

Next, we engineered a molecular network in which the upstream TBP input is processed into the downstream regulation of the proteolytic activity of thrombin (Figure 4c), a protein involved in blood coagulation by cleaving soluble fibrinogen into insoluble fibrin.[30] Its proteolytic activity can be inhibited by a 15-mer DNA aptamer that binds to the fibrinogen-interacting site with nanomolar affinity.[31] Inspired by the molecular design proposed by Ikebukuro and co-workers,[32] we have engineered a thrombin DNA aptamer equipped with a stem-loop handle that allows for controlling the aptamer folding and therefore its inhibitory activity (Figure 4c and SI12). We incorporated a DNA sequence complementary to this loop portion into the structure of a TBP-responsive translator, hereafter referred to as TBP-Thrombin-Translator. Upon binding of TBP, this translator undergoes structural conversion and exposes the active input strand: this causes abrogation of the inhibitory activity of the aptamer by inducing its unfolding through opening of the stem-loop handle (Figure 4c and SI12). The kinetics of thrombin proteolysis was followed by measuring the increase in the scattering of light after fibrinogen (1 mg mL^{-1}) was added to a solution of thrombin (1 nM).[33] Our aptamer structure (50 nM) induced significant inhibition of the enzymatic activity upon binding to thrombin, delaying of ca. 14 minutes the time necessary to obtain half of the maximum signal (Figure SI12). After testing our biomolecular network using a model DNA hairpin input (Figure SI12), we could effectively regulate the activity of thrombin using TBP (300 nM), as demonstrated by the significant acceleration of the coagulation process compared to that obtained in a control experiment (Figure 4d).

Conclusion

Synthetic DNA-based transducers have been previously designed to mediate artificial communication between proteins that are not natural partners.[4] Our study expands on this concept and proposes new design rules that will allow many other DNA-binding proteins to be utilized as molecular inputs guiding DNA computation and programming. We reported here the rational design of synthetic DNA translators responsive to specific DNA-binding proteins that allow protein-controlled actuation of nucleic acid-based molecular networks. This strategy can be used to trigger toehold-mediated strand displacement reactions and to establish artificial protein–RNA and protein–protein communication mediated by DNA-based operations. We therefore envision that many more additional complex tasks may be performed following this approach. Our results suggest that quantitative

detection of DNA-binding proteins may be achieved by coupling a specific DNA translator to molecular amplification systems or to other sensing modalities, such as electrochemical platforms or CRISPR-Cas-based technologies.[13,34] Operating in a reversible manner, that is, recycling a functional DNA translator by controlling its displacement from a bound protein, would also be appealing for performing multiple rounds of molecular recognition-transduction, thus expanding the functionality of the system over time. Controlling 3D self-assembly[35,36] and processing biomolecular information through higher-order circuits may also be carried out through a rational design of the coupled downstream system, including the creation of artificial feedback loops that would allow a fine temporal tuning of the molecular operations[37] and may pave the way to a wide range of new applications in synthetic biology, DNA nanotechnology and life sciences.

Acknowledgements

This project received funding from the European Union's Horizon 2020 research and innovation program under the Marie Skłodowska-Curie grant agreement No 704120 ("MIR-NANO", A.B.) and No 843998 ("DNA-bots", T.P.). The work was also supported by Associazione Italiana per la Ricerca sul Cancro, AIRC (project n. 21965) (F.R.) and by the European Research Council, ERC (Consolidator Grant project n. 819160) (F.R.). A.B. was supported by Fondazione Umberto Veronesi.

Conflict of interest

The authors declare no conflict of interest.

Keywords: aptamers · DNA strand displacement · DNA-binding proteins · dynamic DNA nanotechnology · synthetic biology

[1] G. Badis, M. F. Berger, A. A. Philippakis, S. Talukder, A. R. Gehrke, S. A. Jaeger, E. T. Chan, G. Metzler, A. Vedenko, X. Chen, et al., *Science* **2009**, *324*, 1720 – 1723.
[2] N. C. Seeman, H. F. Sleiman, *Nat. Rev. Mater.* **2017**, *3*, 17068.
[3] Y. Hu, C. M. Niemeyer, *Adv. Mater.* **2019**, *31*, 1806294.
[4] R. Peri-Naor, T. Ilani, L. Motiei, D. Margulies, *J. Am. Chem. Soc.* **2015**, *137*, 9507 – 9510.
[5] D. Y. Zhang, G. Seelig, *Nat. Chem.* **2011**, *3*, 103 – 113.
[6] T. Fu, Y. Lyu, H. Liu, R. Peng, X. Zhang, M. Ye, W. Tan, *Trends Biochem. Sci.* **2018**, *43*, 547 – 560.
[7] L. Qian, E. Winfree, J. Bruck, *Nature* **2011**, *475*, 368 – 372.
[8] B. Groves, Y.-J. Chen, C. Zurla, S. Pochekailov, J. L. Kirschman, P. J. Santangelo, G. Seelig, *Nat. Nanotechnol.* **2016**, *11*, 287 – 294.
[9] F. Wang, H. Lv, Q. Li, J. Li, X. Zhang, J. Shi, L. Wang, C. Fan, *Nat. Commun.* **2020**, *11*, 121.
[10] J. Lloyd, C. H. Tran, K. Wadhwani, C. Cuba Samaniego, H. K. K. Subramanian, E. Franco, *ACS Synth. Biol.* **2018**, *7*, 30 – 37.
[11] M. Rossetti, A. Bertucci, T. Patino, L. Baranda Pellejero, A. Porchetta, *Chem. Eur. J.* **2020**, https://doi.org/10.1002/chem.202001660.
[12] F. Li, H. Zhang, Z. Wang, X. Li, X.-F. Li, X. C. Le, *J. Am. Chem. Soc.* **2013**, *135*, 2443 – 2446.
[13] Y. Tang, Y. Lin, X. Yang, Z. Wang, X. C. Le, F. Li, *Anal. Chem.* **2015**, *87*, 8063 – 8066.
[14] A. Porchetta, R. Ippodrino, B. Marini, A. Caruso, F. Caccuri, F. Ricci, *J. Am. Chem. Soc.* **2018**, *140*, 947 – 953.
[15] W. Engelen, L. H. H. Meijer, B. Somers, T. F. A. de Greef, M. Merkx, *Nat. Commun.* **2017**, *8*, 14473.
[16] S. Ranallo, D. Sorrentino, F. Ricci, *Nat. Commun.* **2019**, *10*, 5509.
[17] T. Heyduk, E. Heyduk, *Nat. Biotechnol.* **2002**, *20*, 171 – 176.
[18] A. Vallée-Bélisle, A. J. Bonham, N. O. Reich, F. Ricci, K. W. Plaxco, *J. Am. Chem. Soc.* **2011**, *133*, 13836 – 13839.
[19] A. J. Bonham, K. Hsieh, B. S. Ferguson, A. Vallée-Bélisle, F. Ricci, H. T. Soh, K. W. Plaxco, *J. Am. Chem. Soc.* **2012**, *134*, 3346 – 3348.
[20] A. Bertucci, J. Guo, N. Oppmann, A. Glab, F. Ricci, F. Caruso, F. Cavalieri, *Nanoscale* **2018**, *10*, 2034 – 2044.
[21] F. Praetorius, H. Dietz, *Science* **2017**, *355*, eaam5488.
[22] A. Vallée-Bélisle, F. Ricci, K. W. Plaxco, *Proc. Natl. Acad. Sci. USA* **2009**, *106*, 13802 – 13807.
[23] T. Rowlands, P. Baumann, S. P. Jackson, *Science* **1994**, *264*, 1326 – 1329.
[24] a) B. Wang, C. Thachuk, A. D. Ellington, E. Winfree, D. Soloveichik, *Proc. Natl. Acad. Sci. USA* **2018**, *115*, E12182 – E12191; b) T. Song, N. Gopalkrishnan, A. Eshra, S. Garg, R. Mokhtar, H. Bui, H. Chandran, J. Reif, *ACS Nano* **2018**, *12*, 11689 – 11697; c) D. Lysne, K. Jones, A. Stosius, T. Hachigian, J. Lee, E. Graugnard, *J. Phys. Chem. B* **2020**, *124*, 3326 – 3335; d) A. Joesaar, S. Yang, B. Bögels, A. van der Linden, P. Pieters, B. V. V. S. P. Kumar, N. Dalchau, A. Phillips, S. Mann, T. F. A. de Greef, *Nat. Nanotechnol.* **2019**, *14*, 369 – 378.
[25] J. E. Darnell, *Nat. Rev. Cancer* **2002**, *2*, 740 – 749.
[26] S. K. Nair, S. K. Burley, *Cell* **2003**, *112*, 193 – 205.
[27] E. V. Dolgosheina, S. C. Y. Jeng, S. S. S. Panchapakesan, R. Cojocaru, P. S. K. Chen, P. D. Wilson, N. Hawkins, P. A. Wiggins, P. J. Unrau, *ACS Chem. Biol.* **2014**, *9*, 2412 – 2420.
[28] R. J. Trachman, A. Autour, S. C. Y. Jeng, A. Abdolahzadeh, A. Andreoni, R. Cojocaru, R. Garipov, E. V. Dolgosheina, J. R. Knutson, M. Ryckelynck, et al., *Nat. Chem. Biol.* **2019**, *15*, 472 – 479.
[29] W. Zhong, J. T. Sczepanski, *ACS Sens.* **2019**, *4*, 566 – 570.
[30] E. Di Cera, *Mol. Aspects Med.* **2008**, *29*, 203 – 254.
[31] L. C. Bock, L. C. Griffin, J. A. Latham, E. H. Vermaas, J. J. Toole, *Nature* **1992**, *355*, 564 – 566.
[32] W. Yoshida, K. Sode, K. Ikebukuro, *Biochem. Biophys. Res. Commun.* **2006**, *348*, 245 – 252.
[33] Y.-C. Shiang, C.-C. Huang, T.-H. Wang, C.-W. Chien, H.-T. Chang, *Adv. Funct. Mater.* **2010**, *20*, 3175 – 3182.
[34] a) Y. Dai, Y. Wu, G. Liu, J. J. Gooding, *Angew. Chem. Int. Ed.* **2020**, https://doi.org/10.1002/anie.202005398; *Angew. Chem.* **2020**, https://doi.org/10.1002/ange.202005398; b) P. Sadat Mousavi, S. J. Smith, J. B. Chen, M. Karlikow, A. Tinafar, C. Robinson, W. Liu, D. Ma, A. A. Green, S. O. Kelley, et al., *Nat. Chem.* **2020**, *12*, 48 – 55; c) M. S. Reid, X. C. Le, H. Zhang, *Angew. Chem. Int. Ed.* **2018**, *57*, 11856 – 11866; *Angew. Chem.* **2018**, *130*, 12030 – 12041.
[35] D. Y. Zhang, R. F. Hariadi, H. M. T. Choi, E. Winfree, *Nat. Commun.* **2013**, *4*, 1965.
[36] W. B. Rogers, V. N. Manoharan, *Science* **2015**, *347*, 639 – 642.
[37] a) S. Mukherji, A. van Oudenaarden, *Nat. Rev. Genet.* **2009**, *10*, 859 – 871; b) H. Liu, Q. Yang, R. Peng, H. Kuai, Y. Lyu, X. Pan, Q. Liu, W. Tan, *J. Am. Chem. Soc.* **2019**, *141*, 6458 – 6461.

Manuscript received: June 17, 2020
Revised manuscript received: July 22, 2020
Accepted manuscript online: August 1, 2020
Version of record online: September 2, 2020

